



## Characterization and theoretical analysis of isoporous cycloaliphatic polyurethane membrane for water treatment

Young-Kwon Choi<sup>a</sup>, Seung-Min Park<sup>a</sup>, Sangho Lee<sup>a,\*</sup>, Dahl-Young Khang<sup>b</sup>, Dong-Chan Choi<sup>c</sup>, Chung-Hak Lee<sup>c</sup>

<sup>a</sup>Department of Civil And Environment Engineering, Kookmin University, Jeongneung-gil 77, Seongbuk-gu, Seoul 136-702, Republic of Korea

Tel. +82 2 910 5060; Fax: +82 2 910 8597; email: sanghlee@kookmin.ac.kr

<sup>b</sup>Department of Materials Science and Engineering, Yonsei University, 50 Yonsei-ro, Seodaemun-gu, Seoul 120-749, Republic of Korea

<sup>c</sup>School of Chemical and Biological Engineering, Seoul National University, 1 Gwanak-ro, Gwanak-gu, Seoul 151-742, Republic of Korea

Received 9 March 2013; Accepted 5 April 2013

---

### ABSTRACT

A narrow pore size distribution is critical for most membrane separation processes even though it is difficult to achieve through conventional methods of membrane synthesis such as phase inversion. Although various technologies have been proposed for the preparation of isoporous membranes, few technologies are available for use in water treatment applications. In our previous works, we have prepared isoporous membranes using a novel technique based on soft lithography. A micro pattern of pyramid shape was applied to produce uniform pores. In this work, we aimed at the characterization of these isoporous membranes using both experimental and theoretical methods. The pore size distributions of the membranes were characterized by scanning electron microscopy image analysis. Using this image analysis technique, the pore size ranging from 2.2 to 21.4  $\mu\text{m}$  could be identified. A simple theoretical model was developed to determine the pore size, porosity, and membrane resistance of the isoporous membranes. A preliminary filtration test was also carried out to examine the fundamental properties of the isoporous membranes.

*Keywords:* Membrane characterization; Uniform pore size; Soft lithography; Pore size control; Model

---

### 1. Introduction

Microfiltration membranes are already commonly used in many applications such as water treatment, wastewater treatment and reclamation, and industrial

water production [1]. It is proven to be a competitive treatment when compared with conventional ones [2]. Recently, microfiltration has been recognized as a competitive pre-treatment for reverse osmosis system [3]. The recent global increase in the use of membranes in water application is attributed to

\*Corresponding author.

*Presented at the Fifth Annual International Conference on "Challenges in Environmental Science & Engineering—CESE 2012" Melbourne, Australia, 9–13 September 2012*

several factors, including increased regulatory pressure, exploitation of water resources of lower quality, and shortage of conventional water resources [4].

Currently, membranes produced through phase inversion method are predominantly used for microfiltration [5,6]. These membranes normally have more or less a wide variance in the distribution of pore size, which has disadvantages such as difficulty in precise separation of substances mixture. Moreover, rapid fouling may occur since a larger portion of the liquid passing through the membrane preferentially passes through large pores, leading to fast blockage of these pores.

Accordingly, a few studies have attempted for some time to prepare isoporous membranes, which have a low variance in the distribution of their pore size [7–9]. A representative example is a track-etched membrane, which is created by a chemical treatment of tracks induced from heavy ions irradiation. Nevertheless, track-etched membranes have drawbacks: first, they have defects such as doublet and triplet pores because the ions bombard randomly; second, they have relatively weak mechanical strength because they do not have a surface layer; third, their pore structures are symmetric, leading to low permeability when compared with those of asymmetric membranes.

Recently, we have examined soft lithography as a new method to prepare isoporous microfiltration membranes made of cycloaliphatic polyurethane [10]. A micro pattern of pyramid shape was used to produce uniform pores. As a result, a variety of isoporous membranes could be prepared.

The focus of this paper was to characterize and analyze the structure of the isoporous membranes because the details on the membrane synthesis are provided in our previous works [10,11]. To understand and control the membrane properties, a simple

theoretical model was developed and applied, which allows the prediction of pore size, porosity, and membrane resistance. In addition, a preliminary filtration test was also conducted to verify if these membranes can be used for water treatment.

## 2. Materials and methods

### 2.1. Isoporous membranes

The isoporous membranes prepared by a technique based on soft lithography were used for the experiments and theoretical analysis in this study. We only give brief information on the membranes here, since details are provided separately [10]. The membranes were made of MINs, which is a mixture of polyacrylate and polyurethane resins. Pyramid micro patterns, which were fabricated by photolithography, were used to create pore structures. Details on these micro patterns are provided elsewhere [12].

The pore size of the isoporous membranes were controlled using a casting knife. The MINs solution was applied on the top of the micro patterns, as illustrated in Fig. 1. The casting knife is used to remove excess MINs and to create pores. By increasing the distance between the top of the pattern and the casting knife, the pore size increases, details are provided separately [11]. The theoretical relationship between the casting knife position and pore size will be discussed later in this paper.

### 2.2. Image analysis

The membranes prepared by this method were examined using scanning electron microscopy (SEM). Then, the SEM images were processed to determine

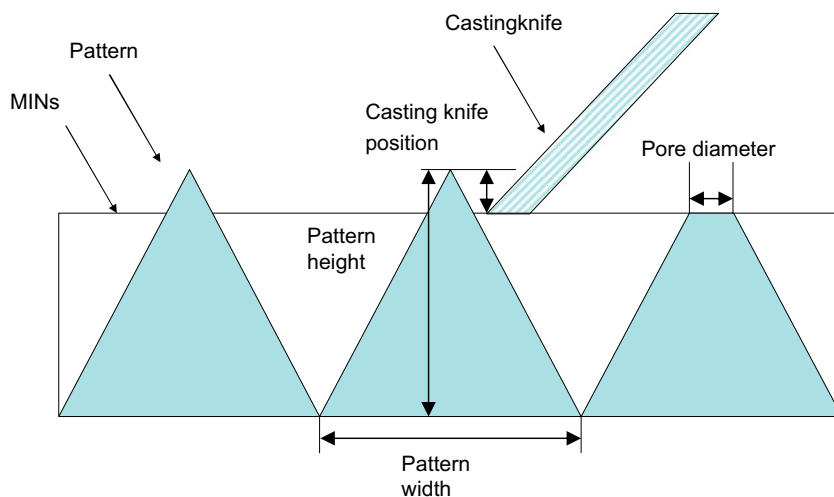


Fig. 1. Mechanism of pore size control by adjusting the position of casting knife.

the porosity, average pore size, and pore size distribution. A code written in Matlab was used to perform segmentation, in which individual pixels in an image are marked as “object” pixels if their value is greater than some threshold value (assuming an object to be brighter than the background) and as “background” pixels otherwise. After segmentation, the properties of pores could be analyzed.

### 2.3. Filtration test

Experiments were performed in batch mode using a stirred cell similar to those which have been widely used for the study of the flux in water research group. The working volume of the stirred cell was 100 mL. The working pressure was provided by a nitrogen cylinder with a gas pressure regulator. The permeate flux was measured using an electronic balance (ARG423, Ohaus, USA) connected to a desktop computer. Pure water permeability was measured using DI water. Surface water from the Han River was used as feed water for preliminary test of flux and rejection.

## 3. Results and discussion

### 3.1. Analysis of pore size distribution and radius ratio

Membranes prepared by the soft lithography method were used for the characterization of their

pore structures. Fig. 2 compares the SEM image of these membranes. In Fig. 3(a), the pores could not be created because the height of the casting knife was higher than that of the micro pattern. As the height of the casting knife decreases, the pore size increases as can be seen in Fig. 3(b)–(d). This suggests that the pore size of these membranes can be easily controlled by adjusting the position of the casting knife.

Using the SEM images shown in Fig. 2, the characteristics of the pores in the three membranes were analyzed based on the image analysis technique. Fig. 3 shows how the images are processed to distinguish pores through the segmentation. Each white area in the image was identified as pore using image analysis functions in Matlab.

The results are shown in Fig. 4, which compares the pore size distributions for the three membranes. The average pore sizes were 2.2, 9.6, and 21.4  $\mu\text{m}$ , respectively. Since the pyramid pattern used in this study has the base length of 28  $\mu\text{m}$  and height of 10  $\mu\text{m}$ , the pore size ranged from 2 to 22  $\mu\text{m}$ . Membranes with smaller pore sizes may be obtained using a smaller pattern. The pore size distributions were narrow when compared with the conventional membranes made by phase inversion techniques. The relative standard deviations were only 0.18, 0.14, and 0.19, respectively.

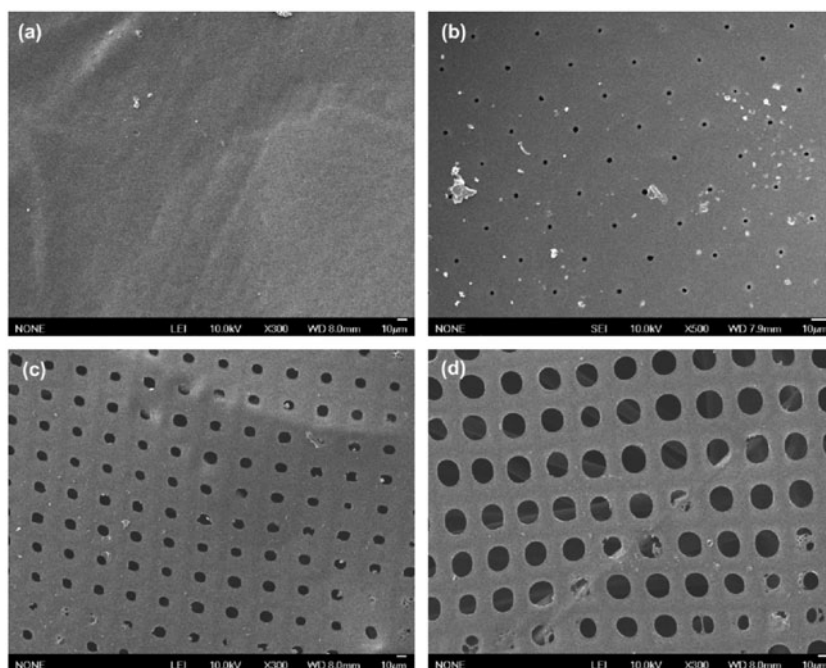


Fig. 2. SEM images of membranes with various pore sizes (a) the height of the casting knife was higher than the height of pattern (b)–(d) pore size increases by adjusting the position of the casting knife.

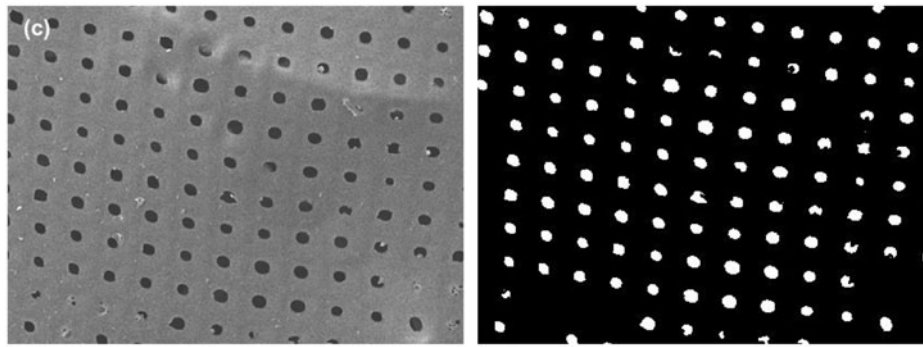


Fig. 3. An example of segmentation of a SEM image of Fig. 2(c).

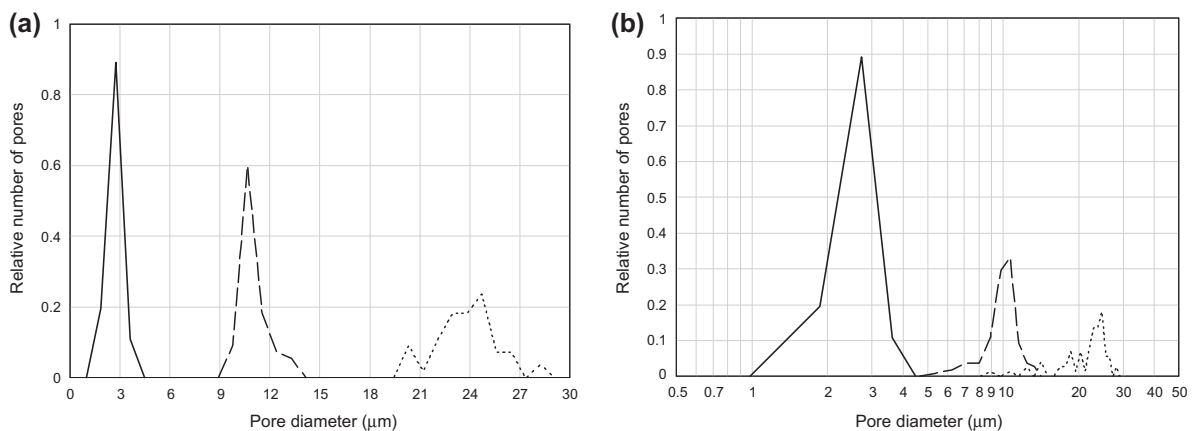


Fig. 4. Pore size distributions of three membranes shown in Fig. 2. (a) Linear  $x$  – Linear  $y$  (b) logarithmic  $x$  – linear  $y$ . (—) membrane in Fig. 2(b); (---) membrane in Fig. 2(c); (···) membrane in Fig. 2(d).

The shapes of the pores were also uniform. As depicted in Fig. 5, the radius ratios, which are defined as the ratio of maximum pore radius to minimum

pore radius, were close to 1.5. This suggests that well-defined pores were developed using this technique.

### 3.2. Theoretical analysis of membrane pore properties

As demonstrated above, there is a close relationship between the position of the casting knife and the average pore size, which is also connected to the porosity and membrane resistance. Accordingly, a theoretical model was developed to understand and predict the properties of these membranes.

First, the pressure drop in a pore is described by the Darcy–Weisbach equation.

$$\Delta P = f_D \frac{L_p}{d_h} \frac{\rho V^2}{2} \quad (1)$$

where  $\Delta P$  is the pressure drop along the pore,  $f_D$  is the dimensionless coefficient called the Darcy friction factor,  $L_p$  is the pore length,  $d_h$  is the hydraulic diameter,  $\rho$  is the fluid density, and  $V$  is the mean velocity of the flow. In laminar flow conditions,  $f_D = 64/Re$

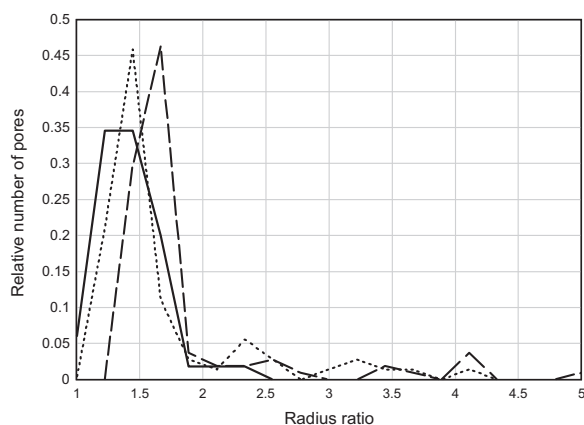


Fig. 5. Distribution of radius ratios for three membranes Fig. 2 (—) membrane in Fig. 2(b); (---) membrane in Fig. 2(c); (···) membrane in Fig. 2(d).

where  $Re$  is the Reynolds number. Thus, the membrane resistance is given by:

$$R_m = \frac{32L_p}{\varepsilon d_h^2} = \frac{8L_p}{\varepsilon r_p^2} \quad (2)$$

where  $r_p = d_h/2$ . Using the pyramid-shaped micro pattern, the following relations apply:

$$L_p = b - L_c \quad (3)$$

$$r_p = \frac{a}{2b}L_c \quad (4)$$

$$\varepsilon = \frac{L_c^2}{b^2} \quad (5)$$

where  $a$  and  $b$  are the base length and height of the pattern, respectively, and  $L_c$  is the distance between the top of the pattern and the position of the casting knife. Finally, the resistance of this membrane, whose pore has a trapezoidal cross-section of pore, is calculated by:

$$R_m = \int_{r_p}^a \frac{8L_p}{\varepsilon(x)x^2} dx \quad (6)$$

Fig. 6 shows the theoretical relationship between the casting knife position and the pore size. As expected, the pore size linearly increases with increasing casting knife position. At the same time, the porosity increases, as demonstrated in Fig. 7. This indicates that the pore size and porosity can be easily controlled by adjusting the position of the casting knife.

Fig. 8 shows how the membrane resistance is affected by the position of the casting knife. Since both the pore size and porosity increase with the casting

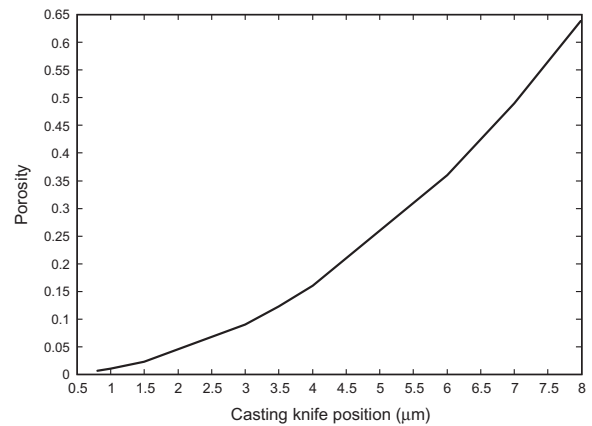


Fig. 7. Simulation of porosity as a function of the casting knife position.

knife position, the membrane resistance decreases, leading to high permeability. It is evident from the graph that the membrane resistance should be reduced to prepare membranes with small pore size. Theoretically,  $R_m$  is about  $4.4 \times 10^{11} \text{ m}^{-1}$  for the membrane with a pore size of  $0.28 \mu\text{m}$ . Nevertheless, it is impossible to prepare this membrane using the current micro pattern because only  $0.1 \mu\text{m}$  of the casting knife position should be applied. A micro pattern with a different dimension is required to create a pore size smaller than  $2 \mu\text{m}$ .

### 3.3. Filtration characteristics

Using an isoporous membrane with a pore size of  $6 \mu\text{m}$ , which was prepared using the same technique, a preliminary test was carried out to examine its fundamental filtration characteristics. Since the membrane permeability was too high, it was difficult to measure

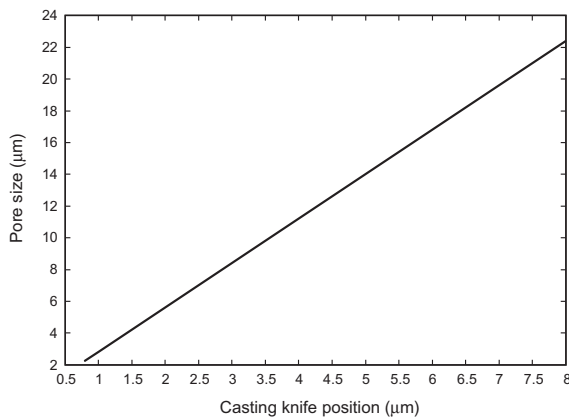


Fig. 6. Simulation of pore size as a function of the casting knife position.

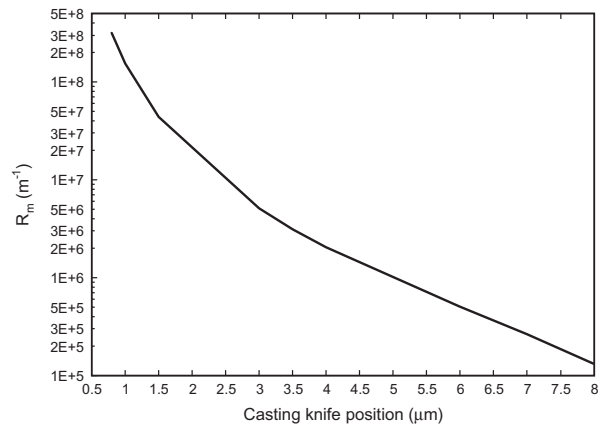


Fig. 8. Simulation of membrane resistance as a function of the casting knife position.

using a stirred cell device. The water permeability was at least higher than 70,000 L/m<sup>2</sup>/h/bar, which was estimated based on water flux measured under applied pressure less than 0.1 bar.

Table 1 compares the water quality parameters for feed water (surface water from the Han River) and permeate from the isoporous membrane. The turbidity removal was about 94% and the UV<sub>abs</sub> removal was about 23%. Considering the pore size (6 μm) of this membrane, they are larger than expected. This may be attributed to the formation of “dynamic membrane layer” on the surface of the membrane. As shown in Fig. 9, the permeability of the membrane rapidly decreases, leading to a constriction of pore size. Accordingly, the rejections for turbidity and organics can be improved. Although the data are not shown, similar flux decline was also observed using track-etched membrane with the pore size of 6 μm. Further works will be required on in-depth analysis of fouling and rejection of this isoporous membrane.

Table 1  
Water quality parameters for feed water and permeate from isoporous membrane ( $d_p=6\ \mu\text{m}$ )

	Water quality parameters	Values
Feed water	UV254 (ABS)	0.048
	Turbidity (NTU)	1.78
Permeate	UV254 (ABS)	0.037
	Turbidity (NTU)	0.098
Rejection (%)	UV254 (ABS)	22.92
	Turbidity (NTU)	94.61

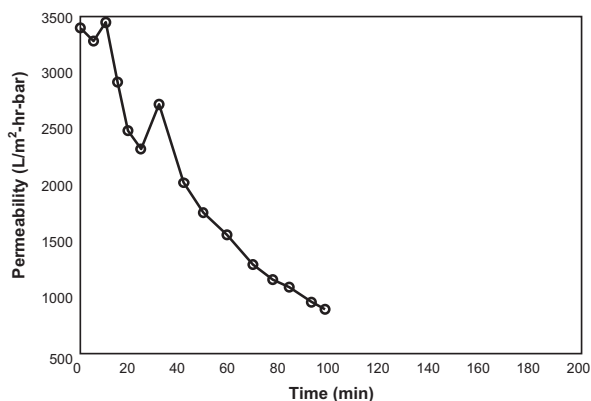


Fig. 9. Dependence of permeate flux on time during the filtration of surface water using isopore membrane ( $d_p=6\ \mu\text{m}$ ).

#### 4. Conclusions

The following conclusions can be drawn from this work:

- (1) The membranes prepared by a technique based on soft lithography were characterized. The results of the image analysis showed that the pore size distribution was narrow. The radius ratios, which are defined as the ratio of maximum pore radius to minimum pore radius, were close to 1.5.
- (2) A theoretical method to predict the pore size, porosity, and membrane resistance was developed to aid the design of these membranes. By increasing the position of the casting knife, the pore size and porosity increase, leading to a reduction in membrane resistance. This implies that the position of the casting knife is a key factor affecting the properties of the membrane.
- (3) A filtration test using a river water sample was conducted to examine the fouling propensity of the isoporous membrane with a pore size of 6 μm. Due to its relatively large pore size, the initial flux was high and the rapid fouling was observed. Further works will be required for better understanding of the filtration characteristics of these membranes.

#### Acknowledgment

This work was supported by the National Research Foundation of Korea Grant funded by the Korean Government (MEST) (NRF-2010-0029061).

#### References

- [1] L.J. Zeman, A.L. Zydney, *Microfiltration and Ultrafiltration: Principles and Applications*, Marcel Dekker, New York, 1996.
- [2] EPA, *Low-Pressure Membrane Filtration for Pathogen Removal: Application, Implementation, and Regulatory Issues*, EPA, Cincinnati, OH, 2001.
- [3] P.H. Wolf, S. Sivers, S. Monti, UF membranes for RO desalination pretreatment, *Desalination* 182(1–3) (2005) 293–300.
- [4] Water scarcity drives membrane market, *Membr. Technol.* 2005(4) (2005) 4.
- [5] R.I. Peinador, J.I. Calvo, P. Prádanos, L. Palacio, A. Hernández, Characterisation of polymeric UF membranes by liquid-liquid displacement porosimetry, *J. Membr. Sci.* 348(1–2) (2010) 238–244.
- [6] M. Ulbricht, Advanced functional polymer membranes, *Polymer* 47 (2006) 2217–2262.
- [7] J.A. Quinn, J.L. Anderson, W.S. Ho, W.J. Petzny, Model pores of molecular dimension: The preparation and characterization of track-etched membranes, *Biophys. J.* 12(8) (1972) 990–1007.
- [8] M. Sára, C. Manigley, G. Wolf, U.B. Sleytr, Isoporous ultrafiltration membranes from bacterial cell envelope layers, *J. Membr. Sci.* 36 (1988) 179–186.

- [9] V. Abetz, V. Filiz, S. Rangou, C. Abetz, A. Jung, K. Buhr, Self-assembled integral asymmetric block copolymer membranes: Structure formation and properties, *Proc. Eng.* 44 (2012) 194–197.
- [10] Chung-Hak Lee, D.C. Choi, Y.J. Won, J.W. Lee, H.R. Chae, I. Kim, S. Lee, Preparation of isopore membrane with low biofouling by lithographic method, IWA Specialist Conference on Particle Separation, Berlin, Germany, June 19, 2012.
- [11] D.C. Choi, Y.J. Won, J.W. Lee, H.R. Chae, Inae Kim, C.H. Lee, Preparation of a membrane for water treatment with low biofouling and narrow pore size distribution by lithographic method, World Water Congress and Exhibition, Busan, Korea, September 17, 2012.
- [12] Y.-J. Won, J. Lee, D.-C. Choi, H.R. Chae, I. Kim, C.-H. Lee, I.-C. Kim, Preparation and application of patterned membranes for wastewater treatment, *Environ. Sci. Technol.* 46 (2012) 11021–11027.